THE JOURNAL OF BIOLOGICAL CHEMISTRY VOL. 287, NO. 5, pp. 3454–3461, January 27, 2012

Conserved YjgF Protein Family Deaminates Reactive Enamine/Imine Intermediates of Pyridoxal 5′-Phosphate (PLP)-dependent Enzyme Reactions*

Received for publication, September 14, 2011, and in revised form, November 16, 2011 Published, JBC Papers in Press, November 17, 2011, DOI 10.1074/jbc.M111.304477

Jennifer A. Lambrecht[1], **Jeffrey M. Flynn, and Diana M. Downs**[2]

From the Department of Bacteriology, University of Wisconsin, Madison, Wisconsin 53706

Background: YjgF proteins are conserved across the three domains of life.
Results: YjgF proteins deaminate unstable products of PLP-dependent enzyme threonine dehydratase by positioning the enamine/imine close to water in the active site.
Conclusion: YjgF is an enamine/imine deaminase and is renamed RidA.
Significance: RidA removes reactive metabolites released by PLP-dependent enzymes before they can damage cellular components.

The YjgF/YER057c/UK114 family of proteins is conserved in all domains of life, suggesting that the role of these proteins arose early and was maintained throughout evolution. Metabolic consequences of lacking this protein in *Salmonella enterica* and other organisms have been described, but the biochemical function of YjgF remained unknown. This work provides the first description of a conserved biochemical activity for the YjgF protein family. Our data support the conclusion that YjgF proteins have enamine/imine deaminase activity and accelerate the release of ammonia from reactive enamine/imine intermediates of the pyridoxal 5′-phosphate-dependent threonine dehydratase (IlvA). Results from structure-guided mutagenesis experiments suggest that YjgF lacks a catalytic residue and that it facilitates ammonia release by positioning a critical water molecule in the active site. YjgF is renamed RidA (reactive intermediate/imine deaminase A) to reflect the conserved activity of the protein family described here. This study, combined with previous physiological studies on *yjgF* mutants, suggests that intermediates of pyridoxal 5′-phosphate-mediated reactions may have metabolic consequences *in vivo* that were previously unappreciated. The conservation of the RidA/YjgF family suggests that reactive enamine/imine metabolites are of concern to all organisms.

The high degree of conservation of the YjgF/YER057c/UK114 family of proteins in all domains of life suggests that the need for these proteins arose early and has been maintained throughout evolution. Structural approaches have not provided significant insights into the physiological role of these proteins (1–9). In contrast, genetic and biochemical analyses of *yjgF* mutants of *Salmonella enterica* suggest that YjgF removes reactive intermediates generated during the course of normal metabolism (10–12). *In vitro* evidence reported by our laboratory supported this hypothesis with the demonstration that *S. enterica* and human YjgF proteins prevented threonine dehydratase-dependent phosphoribosylamine synthesis (13). Results from the previous study suggested that YjgF acted on a product of threonine dehydratase, IlvA, before it was captured by anthranilate phosphoribosyltransferase (TrpD) to generate phosphoribosylamine. This study was initiated to determine the biochemical role of YjgF in the context of these previous observations.

Threonine dehydratase (IlvA; EC 4.3.1.19) is the first enzyme in the isoleucine biosynthetic pathway. IlvA is a pyridoxal 5′-phosphate (PLP)[3]-dependent enzyme that catalyzes the dehydration of threonine to an enamine intermediate (aminocrotonate), which tautomerizes to its imine form (iminobutyrate) and is then non-enzymatically hydrolyzed to form 2-ketobutyrate and free ammonia (14, 15) (Fig. 1). IlvA also dehydrates serine to yield pyruvate via analogous enamine/imine intermediates. It is unclear whether one or both of these reactive nitrogen intermediates exist in solution. Some evidence suggests that a majority of the enamine-to-imine tautomerization occurs while the product is still on the enzyme, suggesting that the most likely intermediate in solution would be the imine tautomer (16–18). In any case, both intermediates are unstable and short-lived, with a combined half-life estimated to be less than 3 min at 30 °C, pH 7–8 (19), or ~4 min at 25 °C, pH 9.7 (20). In fact, the imine derived from serine has a half-life estimated to be 1.5 s (21). Importantly, these numbers represent metabolite half-lives in aqueous solution. In the cellular environment, these intermediates may be far more stable due to molecular crowding and a reduced availability of water (22). It is plausible that persistence of enamine/imine intermediates *in vivo* is problematic due to the highly nucleophilic nature of these metabolites, which may react with and modify cellular targets, thus altering their function.

* This work was supported, in whole or in part, by National Institutes of Health Grant R01 GM095837 from the USPHS (to D. M. D.).
[1] Supported by a Molecular Biosciences Training Grant from the National Institutes of Health (T32 GM07215).
[2] To whom correspondence should be addressed: 1550 Linden Dr., Madison, WI 53706. Tel.: 608-238-0383; E-mail: downs@bact.wisc.edu.

[3] The abbreviations used are: PLP, pyridoxal 5′-phosphate; TAPS, 3-{[2-hydroxy-1,1-bis(hydroxymethyl)ethyl]amino}-1-propanesulfonic acid; CHES, 2-(cyclohexylamino)ethanesulfonic acid; CAPS, 3-(cyclohexylamino)propanesulfonic acid.

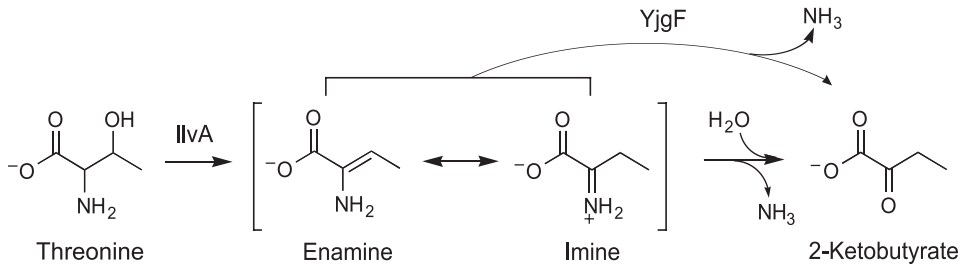

FIGURE 1. **Threonine dehydration and YjgF function.** IlvA dehydrates threonine to generate enamine/imine tautomer intermediates. The imine is hydrolyzed non-enzymatically to form the final products 2-ketobutyrate and ammonia. The data reported under "Results" showed that a biochemical function of YjgF is to catalyze the hydrolysis of these intermediates, thus removing enamine/imine from solution and increasing the rate of production of 2-ketobutyrate.

Data presented herein show that IlvA-generated enamine/imine intermediates serve as substrates for YjgF. Results here show that YjgF family members increased the rate of hydrolysis of the enamine/imine metabolites. This study identified the first conserved biochemical function for the YjgF/YER057c/UK114 family and led to the hypothesis that the role of this ubiquitous family is to accelerate the release of ammonia from enamine/imine intermediates in the low water environment of the cell.

EXPERIMENTAL PROCEDURES

Chemicals—Potassium ferricyanide and other chemicals used in this study were purchased from Sigma-Aldrich. L-[U-^{14}C]Threonine (175 mCi/mmol) was purchased from American Radiolabeled Chemicals Inc.

Bacterial Strains and Plasmids—Pyrococcus furiosus and *Bacillus subtilis* DNA were generously provided by J. Escalante-Semerena. All constructs for overexpression were in vector pET20b+ (Novagen) except for the plasmid containing *chrD* (pET15b (23)) and that containing *rutC* (pCA24N (24)). Site-directed mutagenesis of *yjgF* was performed using the QuikChange II site-directed mutagenesis kit, according to the manufacturer's protocol (Agilent Technologies).

Enzyme Purifications—IlvA and YjgF were purified using C-terminal His_6 tags and nickel ion affinity chromatography, as described previously (13). Variants $YjgF^{Y17F}$, $YjgF^{R105A}$, $YjgF^{E120K}$, and $YjgF^{E120A}$ and protein homologs from *B. subtilis* (YabJ) and *P. furiosus* (PF0668) were purified following the same protocol as for YjgF. Briefly, *Escherichia coli* BL21AI cells carrying the appropriate plasmid were grown to $OD_{650} = 0.7$, expression was induced with 0.2% (w/v) arabinose, and growth continued for 9.5 h at 37 °C. Cells were disrupted with a French pressure cell, and extract was clarified by centrifugation (48,000 × *g* for 45 min). Cell-free extract was applied to nickel-nitrilotriacetic superflow resin, and proteins were purified according to manufacturer's protocol (Qiagen) using column chromatography. Purified protein was concentrated in a 3000 molecular weight cut-off centrifugal filtration unit (Millipore) and then dialyzed using a 10,000 molecular weight cut-off Slide-A-Lyzer dialysis cassette (Thermo Scientific) in 10 mM HEPES, pH 8.0, with 10 mM EGTA, then in 10 mM HEPES, pH 8.0, and lastly in 10 mM HEPES, pH 8.0, with 20% (v/v) glycerol. RutC (YcdK) from *E. coli* was purified from a complete set of *E. coli*, K-12 ORF Archive (ASKA) collection (JW0995), with an N-terminal His_6 tag (24). Cells were grown to $OD_{650} = 0.5$ and induced with 0.2 mM isopropyl-β-D-thiogalactoside and then grown for 9 h more at 37 °C. ChrD was purified with an N-terminal His_6 tag. Cells were grown to $OD_{650} = 0.7$ and induced with 0.2 mM isopropyl-β-D-thiogalactoside and 0.2% (w/v) arabinose and then grown for 9.5 h more at 37 °C. Protein purification procedures for RutC and ChrD were the same as for other YjgF homologs above. All variants and homologs were stably expressed in *S. enterica*, as determined by SDS-PAGE with Coomassie Brilliant Blue staining and/or Western blotting.

Thin-layer Chromatography—Reaction mixes contained 50 mM HEPES, pH 8.0, 10 μM PLP, 0.9 μM IlvA, 50 mM (60 nCi) L-[U-^{14}C]threonine, and 3 μM YjgF when applicable. Reactions were incubated for 2 h at 37 °C, and then radiolabeled compounds were separated by thin-layer chromatography. Spots containing 5 nCi were applied to silica, cellulose, and polyethyleneimine-cellulose plates, and each type of plate was run in each of the following solvent systems: 1-propanol:H_2O, 1:1; methanol:H_2O:pyridine, 20:5:1; 1-butanol:acetic acid:H_2O, 4:2:1; ethanol:ethyl acetate, 9:1; 2-butanol:pyridine:acetic acid:H_2O, 39:34:10:26; 1-butanol:1-propanol:acetic acid:H_2O, 3:1:1:1. The positions of radioactive spots were detected using a Cyclone Storage phosphor screen (Packard Instrument Co.) and a Typhoon FLA 9000 scanner (GE Healthcare). In all solvent/plate combinations, a single ^{14}C-labeled product with the same retention factor as 2-ketobutyrate was detected.

Mass Spectral Analysis—Reactions containing 50 mM ammonium bicarbonate, IlvA, and 50 mM threonine, in the presence and absence of YjgF, were incubated for 2 h. The proteins were removed, and the sample was submitted to positive (+) and negative (−) time-of-flight mass spectral analysis, carried out at the University of Wisconsin Biotechnology Center.

Kinetic Assays—2-Ketobutyrate formation was assayed by following absorbance at 230 nm, as described previously (25). Assays contained 50 mM each MES, HEPES, and TAPS (pH 7.5) or TAPS, CHES, and CAPS (pH 9.5) buffer, 10 μM PLP, 0.9 μM IlvA, and 1.6 μM YjgF or YjgF variants/homologs when applicable. (Assays were also performed in the absence of additional PLP with no change in results.) Substrate threonine or serine was added to begin reactions, and concentrations were varied as indicated. Each reaction was performed in a 200-μl final volume and assayed continuously in a quartz 96-well plate using a SpectraMax Plus (Molecular Devices) at room temperature (22 °C). Initial rates were calculated from the change in $A_{230\ nm}$ over the first 30 s (pH ≤ 9.0) or over 30–60 s (pH > 9.0). Data

were plotted using GraphPad Prism 4.0b, and curves were generated using the Michaelis-Menten equation.

pH Titration—pH titrations were performed with mixtures of the following buffers, each at 50 mM: MES, HEPES, and TAPS (pH ≤ 8.6) or TAPS, CHES, and CAPS (pH ≥ 8.3) (26). In reactions carried out at pH values greater than 9.0 without YjgF, a 30-s burst phase was observed before the reaction velocities became linear. To accommodate the burst, initial velocities for all reactions above pH 9.0 were calculated from 30 to 60 s. Data were plotted using GraphPad Prism 4.0b.

Assays for Ferricyanide Reduction—Reactions contained 50 mM each TAPS, CHES, and CAPS buffer, pH 9.5, 10 μM PLP, 0.9 μM IlvA, and 1.6 μM YjgF when applicable. Ferricyanide was added to a final concentration of 1, 2, or 5 mM as indicated. Reduction of ferricyanide was monitored continuously at 420 nm in a 96-well quartz plate, as described previously (20). Because ferricyanide also absorbs at 230 nm, 2-ketobutyrate concentrations in these reactions were determined by 2,4-dinitrophenylhydrazine derivatization, as described (27).

RESULTS

YjgF Increases Rate of 2-Ketobutyrate Formation from Threonine—Results from thin-layer chromatography experiments showed the formation of a single product in reaction mixtures containing IlvA and threonine. The presence of YjgF did not yield an additional product. The single product was verified as 2-ketobutyrate using time-of-flight mass spectrometry (expected *m/z*, 101.0245; observed *m/z*, 101.0248).

The initial rates of 2-ketobutyrate formation by IlvA were determined with and without YjgF by following absorbance at 230 nm in a continuous assay (25). The presence of YjgF in the reaction mix significantly increased the rate of 2-ketobutyrate formation (Fig. 2*A*). At pH 7.5, with 15 mM threonine as substrate, the initial rate of 2-ketobutyrate formation was nearly 2-fold higher in the presence of YjgF when compared with IlvA alone, whereas at pH 9.5, YjgF stimulated the initial rate 4–5-fold (Fig. 2*B*). YjgF and IlvA proteins were present at monomeric concentrations of 1.6 and 0.9 μM, respectively. Because YjgF is a trimer (1, 2) and IlvA is a tetramer (28), the YjgF:IlvA oligomeric ratio in these experiments was ~2:1. Results from the spectrophotometric assay were corroborated by two independent methods that quantified 2-ketobutyrate using a discontinuous assay. Derivatization of 2-ketobutyrate by *o*-phenylenediamine (29) or 2,4-dinitrophenylhydrazine (27) detected an increased rate of 2-ketobutyrate formation when YjgF was present in the reaction mixtures comparable with that observed by following $A_{230\ nm}$.

Activity of YjgF Is Greater at High pH—The pH of the reaction was titrated from 7.0 to 10.0, using MES/HEPES/TAPS buffer for pH ≤8.6 and TAPS/CHES/CAPS buffer for pH ≥8.3 and 15 mM threonine as substrate. The effect of YjgF on the initial rate of 2-ketobutyrate formation was significantly higher with increasing pH (Figs. 2*B* and Fig. 3). The rate increase with increased pH could be attributed in part to a greater stability of the enamine/imine intermediate at high pH (20, 30). Notably, in reactions with IlvA alone at pH values greater than 9.0, a 30-s burst phase was observed before the reaction velocities became linear. To accommodate the burst, initial velocities for all reactions above pH 9.0 were determined from 30 to 60 s instead of from the first 30 s. This burst was not observed in the presence of YjgF. The presence of a burst in the initial velocity of the reaction was consistent with a reactive product inhibiting IlvA.

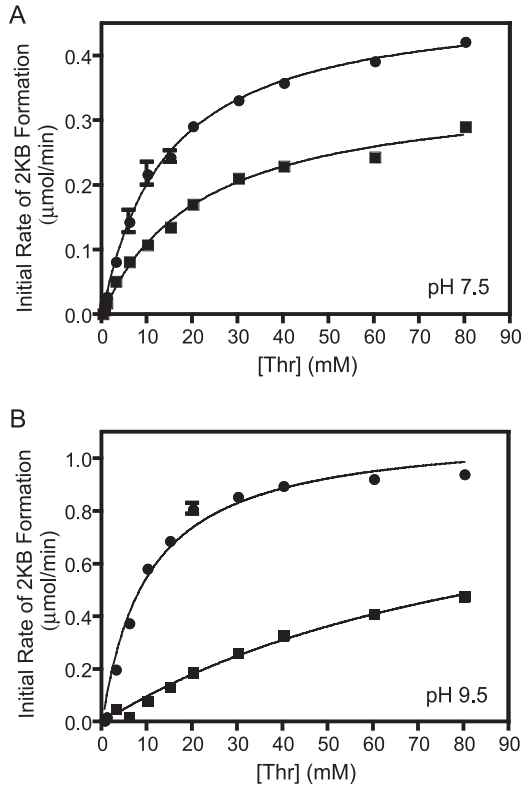

FIGURE 2. **Presence of YjgF changes saturation curve of IlvA.** The initial rate of 2-ketobutyrate (*2KB*) formation *versus* threonine concentration (*[Thr]*); IlvA alone (*squares*); and IlvA + YjgF (*circles*) were measured. *A*, pH 7.5; *B*, pH 9.5. *Error bars* represent S.E. of two replicates; these data are representative of more than five independent experiments.

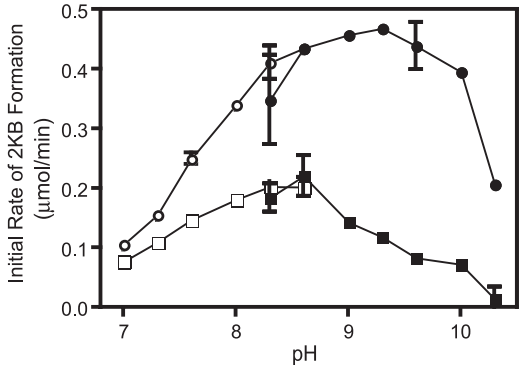

FIGURE 3. **IlvA and YjgF have different pH profiles.** The initial rate of 2-ketobutyrate (*2KB*) formation from 15 mM threonine *versus* pH; IlvA alone (*squares*) and IlvA + YjgF (*circles*) was determined. Buffers are 50 mM each MES/HEPES/TAPS (pH ≤ 8.6; *open symbols*) or 50 mM each TAPS/CHES/CAPS (pH ≥ 8.3; *closed symbols*). *Error bars* represent S.D. of two replicates. These data are representative of two independent experiments.

YjgF Is an Enamine/Imine Deaminase—The availability of enamine/imine metabolites in the IlvA reaction mixes was determined with ferricyanide. Ferricyanide reacts with the enamine/imine metabolites of threonine released from IlvA to produce a decarboxylated non-ketobutyrate product and reduced ferricyanide in a 1:1 ratio (20, 31). Ferricyanide reduction was monitored as a decrease in absorbance at 420 nm. In a

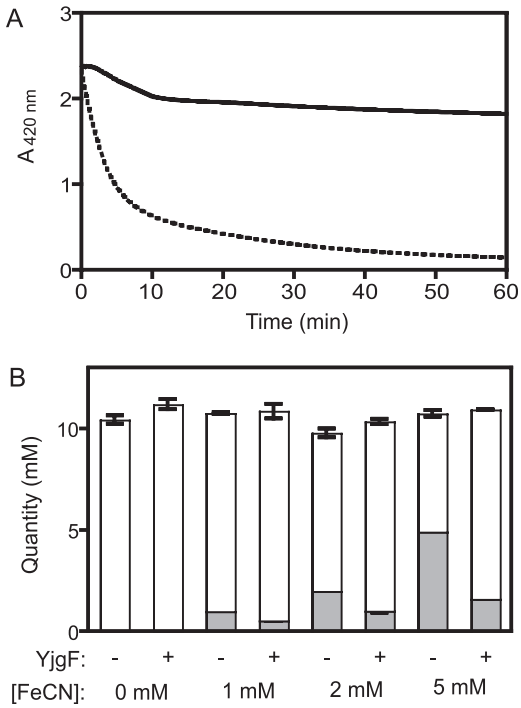

FIGURE 4. **YjgF decreases availability of enamine/imine intermediates of IlvA.** *A*, ferricyanide reduction was followed by absorbance at 420 nm over time. Assays contained 10 mM threonine, 5 mM ferricyanide, and either IlvA alone (*dotted line*) or IlvA with YjgF (*solid line*). *B*, quantities of ferricyanide reduced (*gray bars*) and 2-ketobutyrate produced (*white bars*) in the presence and absence of YjgF after 2 h, with 10 mM threonine and 0, 1, 2, or 5 mM ferricyanide (*FeCN*) as indicated. Ferricyanide concentrations were determined by $A_{420\ nm}$, and 2-ketobutyrate concentrations were determined by 2,4-dinitrophenylhydrazine derivatization (see "Experimental Procedures"). *Error bars* represent S.D. of two replicates; these data are representative of nine and four independent experiments (A and B, respectively).

reaction mix with IlvA, 10 mM threonine, and 5 mM ferricyanide, ferricyanide was rapidly reduced in the first 15 min, with >98% reduced within an hour. In contrast, in the presence of YjgF, ferricyanide reduction occurred slowly, and a plateau was reached after ~10 min, with only 24% of the ferricyanide reduced after 2 h (Fig. 4*A*). These results suggested that the YjgF protein removed the enamine/imine reaction intermediates from solution. A series of reactions was set up that contained IlvA, 10 mM threonine, and different concentrations of ferricyanide in the presence or absence of YjgF. After 2 h, the amounts of 2-ketobutyrate produced and ferricyanide reduced were determined, and the data are shown in Fig. 4*B*. At all concentrations of ferricyanide, YjgF dramatically decreased the amount that was reduced. In the absence of YjgF, the ferricyanide was almost completely reduced, thereby eliminating an equimolar amount of the enamine/imine metabolites and leaving the remainder to be converted to 2-ketobutyrate by hydrolysis in solution. For example, in the presence of 5 mM ferricyanide and IlvA alone, 50% (5 mM) of the reaction intermediates from threonine reduced ferricyanide, whereas the other 50% proceeded to form 2-ketobutyrate. In contrast, when YjgF was present, >90% of the substrate threonine was converted to 2-ketobutyrate, and only ~10% of the reaction intermediates were available to reduce ferricyanide (Fig. 4*B*, *right two bars*). In each reaction condition, the sum of reduced ferricyanide and 2-ketobutyrate was ~10 mM, indicating that all of the threonine provided was consumed by IlvA and accounted for in the two products. Control experiments measuring product formation confirmed that ferricyanide did not affect the initial rate of 2-ketobutyrate formation with or without YjgF. These data support the conclusion that YjgF eliminated enamine/imine intermediates from solution before ferricyanide could react with them.

YjgF Active Site Configuration Is Suggested by Activity of Variant Proteins—The data above suggested that YjgF hydrolyzed an enamine/imine intermediate in a reaction that released ammonia and formed the stable product 2-ketobutyrate. Structural studies and bioinformatic analyses have suggested residues that could comprise an active site of YjgF (Fig. 5*A*). The structure of *E. coli* homolog TdcF (73% identical to *S. enterica* YjgF) with serine, threonine, and the 2-ketobutyrate enol bound implicated residues Arg-105 and Glu-120 in direct binding of substrate (5). Modeling the enamine/imine substrate into this putative active site suggested that Arg-105 formed a bidentate salt bridge with the carboxylic acid of the substrate, as proposed by Burman *et al.* (5). However, based on the activity of YjgF and the apo structure of TdcF containing an ordered water (5), we predicted that Glu-120 did not bind the substrate, but rather formed hydrogen bonds with a water molecule in the active site (Fig. 5*B*). In this scenario, the hydroxyl group of Tyr-17 would stabilize the imine nitrogen. This conformation would place the water <2 Å from C2 of the substrate, and the hydrogen bond between the Tyr-17 and the imine nitrogen would draw electron density away from C2, making the attack by water more favorable (Fig. 5*B*).

Variants of *S. enterica* YjgF were generated to probe the active site mechanism. Four stable YjgF variants ($YjgF^{Y17F}$, $YjgF^{R105A}$, $YjgF^{E120K}$, and $YjgF^{E120A}$) were purified and assayed. The activity of each variant was determined as a ratio of the initial rate of 2-ketobutyrate formation with/without the YjgF protein. The data in Fig. 6 showed that all four variants were defective, with $YjgF^{R105A}$ having the lowest activity. None of the mutations completely eliminated activity. Additionally, $YjgF^{R105A}$ was the only variant that still exhibited burst kinetics. These results are consistent with the model that the role of the active site is to bring the imine and water together to facilitate the attack by water and release of ammonia. This interpretation is consistent with the dominant role of Arg-105 as this residue would hold the imine in place. An alternative model suggesting that Glu-120 had an acid/base role in activating the water molecule was eliminated by the behavior of variants $YjgF^{E120K}$ and $YjgF^{E120A}$. The activity remaining in both variants indicated that Glu-120 was not an essential catalytic residue. These data further suggested that the Glu-120 residue was critical for the increased activity of the YjgF protein at higher pH. Each of the four variants, with the exception of $YjgF^{R105A}$, complemented a *yjgF* mutant defect *in vivo*. This result emphasized the importance of the Arg-105 residue and suggested that the decrease in activity of this variant *in vitro* was physiologically relevant.

YjgF Increased Rate of Pyruvate Formation from IlvA and Serine—IlvA catalyzes the dehydration of serine to generate pyruvate via the corresponding enamine and imine intermediates (15, 32). Pyruvate formation from IlvA and serine was measured at pH 9.5 by following $A_{230\ nm}$ in the presence and

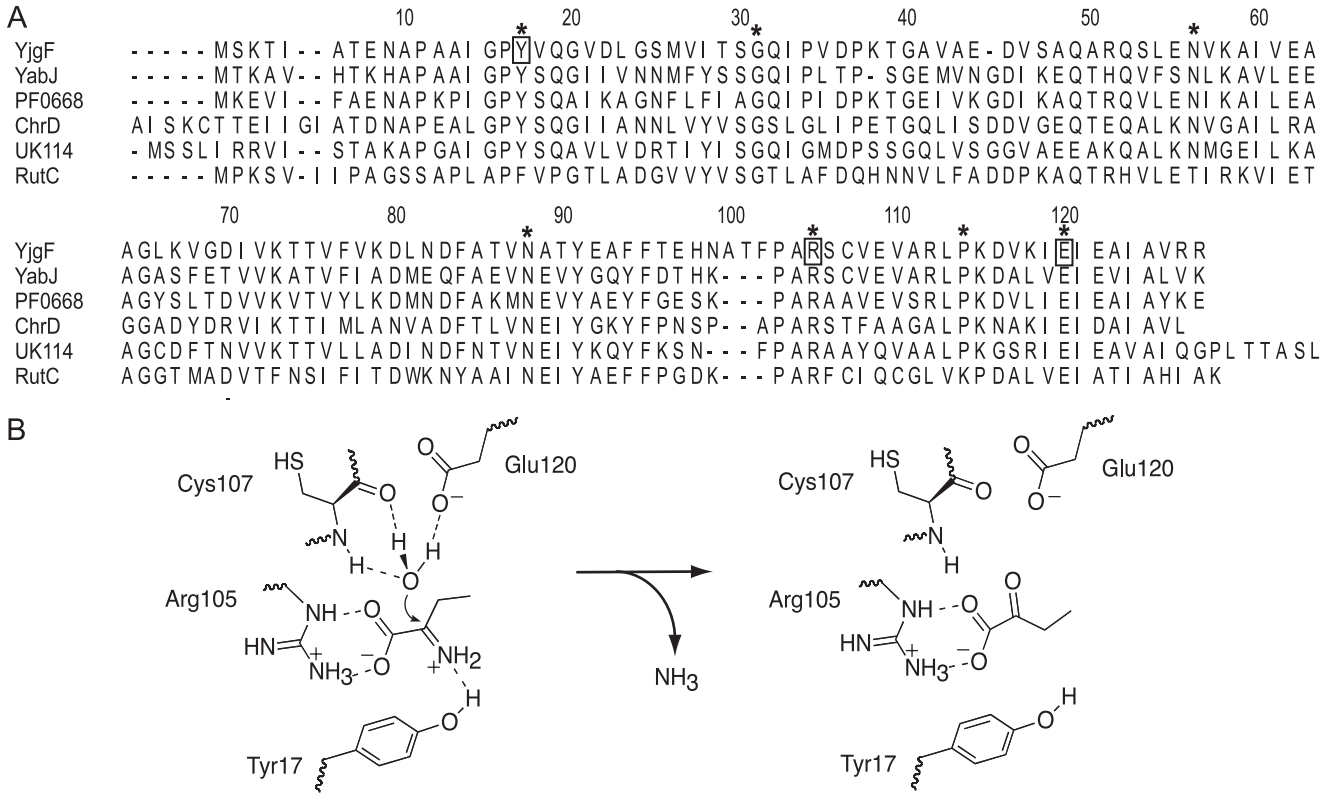

FIGURE 5. **Alignment of family members and proposed mechanism for YjgF.** *A*, amino acid sequences of YjgF family members assayed in this study were aligned using CLUSTALW (45). The numbering of residues is based on the *S. enterica* YjgF sequence. YjgF is from *S. enterica*; YabJ is from *B. subtilis*; PF0668 is from *P. furiosus*; ChrD is from *C. sativus*; UK114 is from *H. sapiens*; and RutC is from *E. coli* K12. *Boxed residues* in the *S. enterica* sequence indicate amino acids mutated in this study. *Asterisks* indicate residues that are invariant among high identity family members (9) and have been predicted to be involved in active site structure or catalysis (5). *B*, a reaction scheme for the deamination of iminobutyrate by YjgF. The backbone of Cys-107 and the side chain of Glu-120 hydrogen-bond with water, whereas the side chain of Arg-105 forms a salt bridge with the carboxyl group of the substrate and the Tyr-17 hydroxyl group hydrogen bonds with the imine nitrogen. This setup facilitates the attack of water on C2 of the imine. Then a rearrangement occurs, releasing the products ammonia and 2-ketobutyrate.

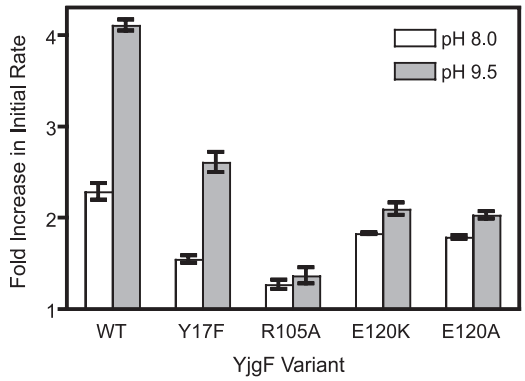

FIGURE 6. **Activity of YjgF variants.** Standard assays contained 15 mM threonine in 50 mM HEPES, pH 8.0 (*white bars*) or CHES, pH 9.5 (*gray bars*), with 0.9 μM IlvA and the indicated YjgF protein (all variants present at 1.6 μM). Activity of YjgF is represented as the -fold increase in the rate of 2-ketobutyrate formation over the rate of IlvA alone (set to 1). *Error bars* represent S.D. of three replicates. Data are representative of three independent experiments.

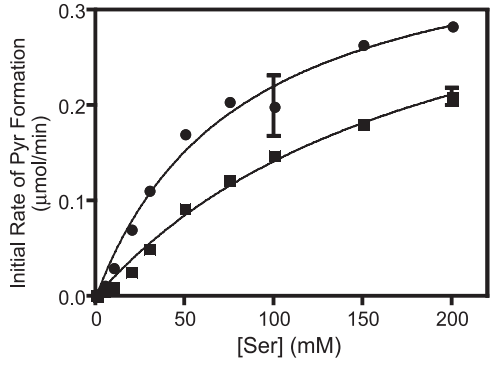

FIGURE 7. **A serine-derived metabolite is another substrate for YjgF.** Initial rate of pyruvate (*Pyr*) formation *versus* serine concentration (*[Ser]*) at pH 9.5; IlvA alone (*squares*) and IlvA + YjgF (*circles*) were measured. *Error bars* represent S.E. of two replicates. Data are representative of three independent experiments.

absence of YjgF. Like 2-ketobutyrate formation, the rate of pyruvate formation was 2.2-fold faster (at 30 mM serine) in the presence of YjgF (Fig. 7). This result identified a second substrate for YjgF and was consistent with the active site configuration proposed in Fig. 5, which did not implicate residues to bind C3 or C4 present in the enamine/imine derived from threonine.

Enamine/Imine Deaminase Activity Is Encoded in YjgF Homologs from Diverse Organisms—Homologs of YjgF from *B. subtilis* (YabJ; 50% identity), *P. furiosus* (PF0668; 56% identity), *Cucumis sativus* (ChrD; 42% identity), *Homo sapiens* (UK114; 45% identity), and *E. coli* (RutC/YcdK; 29% identity) were assayed for 2-ketobutyrate formation activity (see Fig. 5*A* for sequence alignment). Each of the five homologs significantly increased the rate of 2-ketobutyrate formation from threonine over that of IlvA alone (Fig. 8). Low identity homolog RutC had

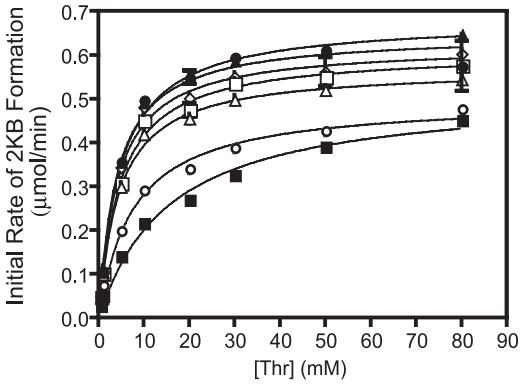

FIGURE 8. **Deaminase activity of YjgF is conserved across domains.** Initial rate of 2-ketobutyrate (*2KB*) formation *versus* threonine concentration (*[Thr]*) at pH 8.0 with diverse YjgF homologs (all present at 1.6 μM). IlvA alone (*closed squares*), IlvA + *S. enterica* YjgF (*closed circles*), IlvA + *B. subtilis* YabJ (*closed triangles*), IlvA + *H. sapiens* UK114 (*open squares*), IlvA + *C. sativus* ChrD (*open triangles*), IlvA + *P. furiosus* PF0668 (*open diamonds*), and IlvA + *E. coli* RutC (*open circles*) were measured. *Error bars* represent S.E. of two replicates. These data are representative of two independent experiments.

less activity in this assay than the higher identity homologs. This result was consistent with the reduced activity of the YjgF^{Y17F} variant because RutC also has a phenylalanine at the residue corresponding to Tyr-17 in the wild-type protein (Fig. 5*A*).

DISCUSSION

The YjgF/YER057c/UK114 family of proteins is broadly conserved and found in all domains of life. Past work, primarily in *S. enterica*, suggested that the diverse phenotypes of *yjgF* mutants reflected a global metabolic role for this protein family (11–13, 33). The results reported herein define an enamine/imine deaminase activity associated with the YjgF protein and homologs from all domains of life, including humans. This is the first report of a conserved biochemical activity for this ubiquitous family. The activity described here for YjgF proteins suggests that the role of these proteins *in vivo* is to accelerate the release of ammonia from enamine/imine intermediates generated by PLP-dependent dehydratases. The conservation of YjgF proteins may be an indication that the low free-water environment of the cell extends the half-life of these metabolites. These findings have implications for reactions that use solvent water to complete product formation and may indicate a need for accessory proteins that were not anticipated from past *in vitro* work performed in aqueous solutions.

Proposed Active Site Configuration for YjgF Function—Previous structural studies (5, 9) and the biochemical analyses of YjgF variants performed here support a mechanism for YjgF catalytic activity (Fig. 5*B*). We propose that Arg-105 forms a bidentate salt bridge with the carboxylic acid of the imine/enamine substrate, consistent with a previous structure containing the 2-ketobutyrate enol in the active site (5). In this scenario, the hydroxyl group of Tyr-17 stabilizes the nitrogen of the substrate, drawing electron density and activating the substrate for nucleophilic attack by a water molecule stabilized by Glu-120 and the backbone of Cys-107. Evidence for this placement of water was found in the apo structure of TdcF, where an ordered water was within an adequate distance to hydrogen-bond to Glu-120 and Cys-107 (5). After the nucleophilic attack, a rearrangement could displace ammonia and generate 2-ketobutyrate. The decreased activities of variants YjgF^{Y17F}, YjgF^{R105A}, YjgF^{E120A}, and YjgF^{E120K} are consistent with this general reaction scheme. Arg-105 is a critical residue, responsible for binding the substrate and required to complement a *yjgF* mutant defect *in vivo*. Significantly, the YjgF^{R105A} variant had the biggest effect on *in vitro* activity and was the only variant that failed to eliminate the burst kinetics observed in high pH reactions with IlvA alone. Tyr-17 played a significant role in stabilizing substrate, as indicated by ~50% reduction in activity at both pH levels when this residue was substituted. The behavior of the YjgF^{E120A} and YjgF^{E120K} variants indicates that Glu-120 has a more significant role at higher pH, where enamine/imines are known to be more stable (20, 30). This result could reflect a need to optimally orient the water molecule in the active site for the nucleophilic attack. Although altering the active site residues led to decreased activities, no mutation completely abolished function. This result suggests that YjgF acts to place water and reactive enamine/imine substrates in close proximity to facilitate a more rapid release of ammonia and does so without a catalytic residue. In the cellular environment, where available water may be limiting, the impact of YjgF proteins is expected to be significant in facilitating stable product formation.

Diversity among YjgF Homologs—YjgF homologs from five diverse organisms were found to have the same activity as the *S. enterica* protein when measured in assays described here and previously (13). The diversity of homologs that have activity in the assays minimizes the possibility that a protein-protein interaction is required for YjgF activity. Consistent with the activity demonstrated here, some enzymes that participate in other enamine deamination reactions can be defined as low identity members of the YjgF family (25–30% identical to *S. enterica*). In *Pseudomonas pseudoalcaligenes*, a YjgF-like protein was shown to deaminate the short-lived enamine 2-aminomuconate to 4-oxalocrotonic acid during the degradation of nitrobenzene (34), and the same reaction has been reported for homologs NbzE in nitrobenzene-degrading *Pseudomonas putida* HS12 (35) and AmnD in *Pseudomonas* sp. AP-3 (36). In *Burkholderia cepacia*, a YjgF homolog increased the rate of 2-aminomuconate deamination more than 70-fold when compared with non-enzymatic hydrolysis in a tryptophan degradation pathway (37). It is likely that this enhanced catalysis was due to an enamine deamination similar to that described here. Finally, in *Bordetella* sp. strain 10d, AhdB deaminates 2-amino-5-carboxymuconic 6-semialdehyde, an unstable enamine intermediate (38, 39). Interestingly, *rutC* in *E. coli* is included in a pyrimidine degradation operon, encoding a pathway that proceeds via the unstable enamine intermediate 3-aminoacrylate (40). Although the biochemical role of RutC in this pathway was not defined, our data support the prediction that RutC acts on the unstable enamine intermediate.

In addition to RutC, other YjgF family members are encoded within operons dedicated to a specific metabolic pathway. Often these operons contain a dedicated threonine and/or serine dehydratase. For example, the anaerobically expressed *tdc* operon in *E. coli* (41) and the alanylclavam biosynthetic operon

in *Streptomyces clavuligerus* (42) have genes encoding both threonine/serine dehydratases and YjgF homologs. These genomic organizations are consistent with the model that the YjgF proteins act on short-lived reactive metabolites generated during specific metabolic processes.

Change to Genome Annotation and Significance of Rid Proteins—We have renamed *yjgF* as *ridA* (reactive intermediate/imine deaminase A) to reflect the biochemical activity of the gene product and to meet the standards of gene nomenclature. This study determined that RidA acts on reaction intermediates from a PLP-dependent enzyme, threonine dehydratase, to increase the rate of product formation above the solvent-mediated reaction. This activity has two anticipated consequences *in vivo*: 1) increasing the hydration rates in low water environment to improve product generation and 2) removing reactive metabolites. We suggest that the diverse phenotypes described for *ridA* (*yjgF*) mutants in *S. enterica* (10, 11, 13, 33) result from the accumulation of enamine/imine intermediates and that the nucleophilic nature of these metabolites allows them to react with and modify cellular targets, altering their function. The plausibility of this scenario is supported by literature reports that the aminoacrylate enamine derived from serine can inactivate a number of enzymes *in vitro* (43, 44). Thus, it is reasonable to suggest that Rid proteins evolved to facilitate the release of ammonia from enamine/imine intermediates generated during normal metabolism, and as a result, reduce the impact of these reactive metabolites on cellular components.

Acknowledgments—We thank W. W. Cleland and Shelley Copley for discussions regarding preparation of this manuscript and Tonya Zeczycki for assistance with kinetic analyses. We thank Michael Thomas and Jorge Escalante-Semerena for critical reading of the manuscript. We also thank Benjamin Bice and Melissa Christopherson, who provided purified IlvA and UK114, respectively, George Schmitz for cloning pET20b-yabJ, Tiffany Lowe for cloning pET20b-PF0668, and Marianna Ovadis and Alexander Vainstein (Hebrew University of Jerusalem, Israel) for kindly providing the pET15b-chrD construct.

REFERENCES

1. Volz, K. (1999) A test case for structure-based functional assignment: the 1.2 A crystal structure of the yjgF gene product from Escherichia coli. *Protein Sci.* **8,** 2428–2437
2. Sinha, S., Rappu, P., Lange, S. C., Mäntsälä, P., Zalkin, H., and Smith, J. L. (1999) Crystal structure of Bacillus subtilis YabJ, a purine regulatory protein and member of the highly conserved YjgF family. *Proc. Natl. Acad. Sci. U.S.A.* **96,** 13074–13079
3. Miyakawa, T., Lee, W. C., Hatano, K., Kato, Y., Sawano, Y., Miyazono, K., Nagata, K., and Tanokura, M. (2006) Crystal structure of the YjgF/YER057c/UK114 family protein from the hyperthermophilic archaeon *Sulfolobus tokodaii* strain 7. *Proteins* **62,** 557–561
4. Deriu, D., Briand, C., Mistiniene, E., Naktinis, V., and Grütter, M. G. (2003) Structure and oligomeric state of the mammalian tumour-associated antigen UK114. *Acta Crystallogr. D. Biol. Crystallogr.* **59,** 1676–1678
5. Burman, J. D., Stevenson, C. E., Sawers, R. G., and Lawson, D. M. (2007) The crystal structure of Escherichia coli TdcF, a member of the highly conserved YjgF/YER057c/UK114 family. *BMC Struct. Biol.* **7,** 30
6. Thakur, K. G., Praveena, T., and Gopal, B. (2010) *Mycobacterium tuberculosis* Rv2704 is a member of the YjgF/YER057c/UK114 family. *Proteins* **78,** 773–778
7. Manjasetty, B. A., Delbrück, H., Pham, D. T., Mueller, U., Fieber-Erdmann, M., Scheich, C., Sievert, V., Büssow, K., Niesen, F. H., Weihofen, W., Loll, B., Saenger, W., Heinemann, U., and Neisen, F. H. (2004) Crystal structure of *Homo sapiens* protein hp14.5. *Proteins* **54,** 797–800
8. Deaconescu, A. M., Roll-Mecak, A., Bonanno, J. B., Gerchman, S. E., Kycia, H., Studier, F. W., and Burley, S. K. (2002) X-ray structure of *Saccharomyces cerevisiae* homologous mitochondrial matrix factor 1 (Hmf1). *Proteins* **48,** 431–436
9. Parsons, L., Bonander, N., Eisenstein, E., Gilson, M., Kairys, V., and Orban, J. (2003) Solution structure and functional ligand screening of HI0719, a highly conserved protein from bacteria to humans in the YjgF/YER057c/UK114 family. *Biochemistry* **42,** 80–89
10. Christopherson, M. R., Schmitz, G. E., and Downs, D. M. (2008) YjgF is required for isoleucine biosynthesis when *Salmonella enterica* is grown on pyruvate medium. *J. Bacteriol.* **190,** 3057–3062
11. Schmitz, G., and Downs, D. M. (2004) Reduced transaminase B (IlvE) activity caused by the lack of yjgF is dependent on the status of threonine deaminase (IlvA) in *Salmonella enterica* serovar Typhimurium. *J. Bacteriol.* **186,** 803–810
12. Browne, B. A., Ramos, A. I., and Downs, D. M. (2006) PurF-independent phosphoribosyl amine formation in yjgF mutants of *Salmonella enterica* utilizes the tryptophan biosynthetic enzyme complex anthranilate synthase-phosphoribosyltransferase. *J. Bacteriol.* **188,** 6786–6792
13. Lambrecht, J. A., Browne, B. A., and Downs, D. M. (2010) Members of the YjgF/YER057c/UK114 family of proteins inhibit phosphoribosylamine synthesis *in vitro*. *J. Biol. Chem.* **285,** 34401–34407
14. Chargaff, E., and Sprinson, D. B. (1943) Studies on the mechanism of deamination of serine and threonine in biological systems. *J. Biol. Chem.* **151,** 273–280
15. Phillips, A. T., and Wood, W. A. (1965) The mechanism of action of 5′-adenylic acid-activated threonine dehydrase. *J. Biol. Chem.* **240,** 4703–4709
16. Dunathan, H. C. (1971) Stereochemical aspects of pyridoxal phosphate catalysis. *Adv. Enzymol. Relat. Areas Mol. Biol.* **35,** 79–134
17. Grabowski, R., Hofmeister, A. E., and Buckel, W. (1993) Bacterial L-serine dehydratases: a new family of enzymes containing iron-sulfur clusters. *Trends Biochem. Sci.* **18,** 297–300
18. Davis, L., and Metzler, D. E. (1972) in *The Enzymes* (Boyer, P., ed) Vol. 7, pp. 33–74, Academic Press, New York
19. Flavin, M., and Slaughter, C. (1964) An intermediate trapped by maleimides in a pyridoxal phosphate potentiated enzymatic elimination reaction. *Biochemistry* **3,** 885–893
20. Datta, P., and Bhadra, R. (1978) Biodegradative threonine dehydratase. Reduction of ferricyanide by an intermediate of the enzyme-catalyzed reaction. *Eur. J. Biochem.* **91,** 527–532
21. Hillebrand, G. G., Dye, J. L., and Suelter, C. H. (1979) Formation of an intermediate and its rate of conversion to pyruvate during the tryptophanase-catalyzed degradation of *S-o*-nitrophenyl-L-cysteine. *Biochemistry* **18,** 1751–1755
22. Zhou, H. X., Rivas, G., and Minton, A. P. (2008) Macromolecular crowding and confinement: biochemical, biophysical, and potential physiological consequences. *Annu. Rev. Biophys.* **37,** 375–397
23. Leitner-Dagan, Y., Ovadis, M., Zuker, A., Shklarman, E., Ohad, I., Tzfira, T., and Vainstein, A. (2006) CHRD, a plant member of the evolutionarily conserved YjgF family, influences photosynthesis and chromoplastogenesis. *Planta* **225,** 89–102
24. Kitagawa, M., Ara, T., Arifuzzaman, M., Ioka-Nakamichi, T., Inamoto, E., Toyonaga, H., and Mori, H. (2005) Complete set of ORF clones of *Escherichia coli* ASKA library (a complete set of *E. coli* K-12 ORF archive): unique resources for biological research. *DNA Res.* **12,** 291–299
25. Davis, L. (1965) A spectrophotometric method for the assay of threonine dehydratase. *Anal. Biochem.* **12,** 36–40
26. Good, N. E., Winget, G. D., Winter, W., Connolly, T. N., Izawa, S., and Singh, R. M. (1966) Hydrogen ion buffers for biological research. *Biochemistry* **5,** 467–477
27. Burns, R. O. (1971) L-Threonine deaminase-biosynthetic (*Salmonella typhimurium*). *Methods Enzymol.* **17,** 555–560
28. Zarlengo, M. H., Robinson, G. W., and Burns, R. O. (1968) Threonine deaminase from *Salmonella typhimurium*. II. The subunit structure.

J. Biol. Chem. **243,** 186–191
29. Li, R., and Kenyon, G. L. (1995) A spectrophotometric determination of α-dicarbonyl compounds and its application to the enzymatic formation of α-ketobutyrate. *Anal. Biochem.* **230,** 37–40
30. Feldberg, R. S., and Datta, P. (1971) L-Threonine deaminase of *Rhodospirillum rubrum*. Purification and characterization. *Eur. J. Biochem.* **21,** 438–446
31. Feldberg, R. S., and Datta, P. (1970) Threonine deaminase: a novel activity stain on polyacrylamide gels. *Science* **170,** 1414–1415
32. Wood, W. A., and Gunsalus, I. C. (1949) Serine and threonine deaminases of *Escherichia coli*; activators for a cell-free enzyme. *J. Biol. Chem.* **181,** 171–182
33. Enos-Berlage, J. L., Langendorf, M. J., and Downs, D. M. (1998) Complex metabolic phenotypes caused by a mutation in yjgF, encoding a member of the highly conserved YER057c/YjgF family of proteins. *J. Bacteriol.* **180,** 6519–6528
34. He, Z., and Spain, J. C. (1998) A novel 2-aminomuconate deaminase in the nitrobenzene degradation pathway of Pseudomonas pseudoalcaligenes JS45. *J. Bacteriol.* **180,** 2502–2506
35. Park, H. S., and Kim, H. S. (2000) Identification and characterization of the nitrobenzene catabolic plasmids pNB1 and pNB2 in Pseudomonas putida HS12. *J. Bacteriol.* **182,** 573–580
36. Takenaka, S., Murakami, S., Kim, Y. J., and Aoki, K. (2000) Complete nucleotide sequence and functional analysis of the genes for 2-aminophenol metabolism from *Pseudomonas* sp. AP-3. *Arch. Microbiol.* **174,** 265–272
37. Colabroy, K. L., and Begley, T. P. (2005) Tryptophan catabolism: identification and characterization of a new degradative pathway. *J. Bacteriol.* **187,** 7866–7869
38. Orii, C., Takenaka, S., Murakami, S., and Aoki, K. (2004) A novel coupled enzyme assay reveals an enzyme responsible for the deamination of a chemically unstable intermediate in the metabolic pathway of 4-amino-3-hydroxybenzoic acid in *Bordetella* sp. strain 10d. *Eur. J. Biochem.* **271,** 3248–3254
39. Takenaka, S., Sato, T., Koshiya, J., Murakami, S., and Aoki, K. (2009) Gene cloning and characterization of a deaminase from the 4-amino-3-hydroxybenzoate-assimilating *Bordetella* sp. strain 10d. *FEMS Microbiol. Lett.* **298,** 93–98
40. Kim, K. S., Pelton, J. G., Inwood, W. B., Andersen, U., Kustu, S., and Wemmer, D. E. (2010) The Rut pathway for pyrimidine degradation: novel chemistry and toxicity problems. *J. Bacteriol.* **192,** 4089–4102
41. Sawers, G. (1998) The anaerobic degradation of L-serine and L-threonine in enterobacteria: networks of pathways and regulatory signals. *Arch. Microbiol.* **171,** 1–5
42. Zelyas, N. J., Cai, H., Kwong, T., and Jensen, S. E. (2008) Alanylclavam biosynthetic genes are clustered together with one group of clavulanic acid biosynthetic genes in Streptomyces clavuligerus. *J. Bacteriol.* **190,** 7957–7965
43. Likos, J. J., Ueno, H., Feldhaus, R. W., and Metzler, D. E. (1982) A novel reaction of the coenzyme of glutamate decarboxylase with L-serine *O*-sulfate. *Biochemistry* **21,** 4377–4386
44. Ueno, H., Likos, J. J., and Metzler, D. E. (1982) Chemistry of the inactivation of cytosolic aspartate aminotransferase by serine *O*-sulfate. *Biochemistry* **21,** 4387–4393
45. Thompson, J. D., Higgins, D. G., and Gibson, T. J. (1994) CLUSTAL W: improving the sensitivity of progressive multiple sequence alignment through sequence weighting, position-specific gap penalties, and weight matrix choice. *Nucleic Acids Res.* **22,** 4673–4680